

# NORMALIZED ITERATIVE HARD THRESHOLDING FOR MATRIX COMPLETION\*

JARED TANNER<sup>†</sup> AND KE WEI<sup>‡</sup>

**Abstract.** Matrices of low rank can be uniquely determined from fewer linear measurements, or entries, than the total number of entries in the matrix. Moreover, there is a growing literature of computationally efficient algorithms which can recover a low rank matrix from such limited information; this process is typically referred to as matrix completion. We introduce a particularly simple yet highly efficient alternating projection algorithm which uses an adaptive stepsize calculated to be exact for a restricted subspace. This method is proven to have near-optimal order recovery guarantees from dense measurement masks and is observed to have average case performance superior in some respects to other matrix completion algorithms for both dense measurement masks and entry measurements. In particular, this proposed algorithm is able to recover matrices from extremely close to the minimum number of measurements necessary.

**Key words.** matrix completion, compressed sensing, low rank approximation, alternating projection

**AMS subject classifications.** 15A29, 15A83, 41A29, 65F10, 65J20, 68Q25, 90C26, 93C41

**DOI.** 10.1137/120876459

**1. Introduction.** Data with a known underlying low dimensional structure can often be acquired from fewer measurements than simple dimension counting would suggest. Moreover, there are cases where not only can the measurement process be independent of the data, giving a linear measurement process, but the data can also be recovered using computationally efficient algorithms. For example, in compressed sensing [7, 11, 16], vectors of length  $n$  that have only  $k \ll n$  nonzero entries can often be determined in polynomial time from fewer than  $n$  inner products; for details see [1, 3, 4, 8, 7, 10, 13, 14, 17, 18, 20, 37] and references therein. Similarly,  $m \times n$  matrices with an inherent simplicity can be uniquely determined from  $p < mn$  inner products. A particularly trivial example is the simplicity model of matrices with few nonzero entries, which can be recast as standard compressed sensing by reforming the matrix as an  $mn$  length sparse vector. Another common notion of matrix simplicity is low rank.

An  $m \times n$  matrix,  $X \in \mathbb{R}^{m \times n}$ , has  $\text{rank}(X) = r$  if and only if  $X$  has a singular value decomposition (SVD)  $X = U\Sigma V^*$ , where  $U$  and  $V$  are matrices of size  $m \times r$  and  $n \times r$ , respectively, with orthonormal columns and  $\Sigma$  is a diagonal matrix with nonincreasing and nonzero diagonal entries,  $\sigma_i(X) := \Sigma(i, i)$ . Throughout this manuscript we reserve the notation  $U, \Sigma$ , and  $V$  to denote the SVD of an associated matrix. There is currently a rapidly growing literature examining the acquisition of low rank matrices from what appears naively to be an insufficient amount of information. The manifold of  $m \times n$  matrices of rank  $r$  is  $r(m+n-r)$  dimensional [43], which specifies the minimum number of values needed to uniquely determine such matrices; this minimal  $r(m+n-r)$  number

\*Received by the editors May 8, 2012; accepted for publication (in revised form) February 8, 2013; published electronically October 28, 2013.

<http://www.siam.org/journals/sisc/35-5/87645.html>

<sup>†</sup>School of Mathematics and Maxwell Institute, University of Edinburgh, Edinburgh, UK (jared.tanner@ed.ac.uk). This author's work was supported by the Leverhulme Trust and by the EPSRC grant EP/J020567/1.

<sup>‡</sup>School of Mathematics and Maxwell Institute, University of Edinburgh, Edinburgh, UK (k.wei@sms.ed.ac.uk). This author's work was supported by the China Scholarship Council.

of values is referred to as the oracle rate. Unfortunately the oracle rate requires the ability to request entries of the singular values and vectors, which is impractical. Consider instead acquiring information about the low rank matrix through  $p$  linear measurements of the form

$$(1.1) \quad b_\ell := \mathcal{A}(X)_\ell = \text{trace}(A_\ell^* X) \quad \text{for} \quad \ell = 1, 2, \dots, p.$$

where the  $p$  distinct  $m \times n$  matrices  $A_\ell$  are the sensing matrices making up the operator  $\mathcal{A}(\cdot)$  that maps  $m \times n$  matrices to vectors of length  $p$ . The sensing matrices  $A_\ell$  are typically normalized such that  $\text{trace}(A_\ell^* A_\ell)$  is exactly, or approximately, equal to one. Of particular interest is the case where the sensing matrices  $A_\ell$  have only one nonzero entry, which corresponds to directly measuring entries of  $X$ , often where the set of  $p$  measured entries in  $X$  are drawn uniformly at random from the  $\binom{mn}{p}$  possible choices. When a subset of the matrix entries are directly measured, finding the unknown entries is typically referred to as “matrix completion” [9, 12, 25]. Recovering the desired matrix when the measurement strategy (1.1) involves dense matrices  $\{A_\ell\}_{\ell=1}^p$  lacks a widely agreed moniker; we will refer to recovery of a low rank matrix from both *entry sensing* and *dense sensing* [38] as matrix completion.

This paper considers the following question: What is an efficient algorithm capable of recovering rank  $r$  matrices with  $r$  as large as possible given  $p$ ,  $m$ ,  $n$ , and  $\mathcal{A}(\cdot)$  specified? It is obvious that  $X$  is recoverable from  $p = mn$  entry measurements, as this corresponds to directly measuring each entry in  $X$ . However, as few as  $r(m + n - r)$  measurements may be sufficient as this is the dimensionality of  $m \times n$  rank  $r$  matrices. We compare  $p$  with the maximum number of measurements required,  $mn$ , and the minimum number of measurements,  $r(m + n - r)$ , through *undersampling* and *oversampling ratios*,

$$(1.2) \quad \delta := \frac{p}{mn} \quad \text{and} \quad \rho := \frac{r(m + n - r)}{p},$$

respectively. Remarkably there are computationally efficient algorithms, such as those in [36, 21, 24, 22, 43, 44, 40, 5, 6, 41, 15, 33, 25, 26, 30, 45, 32, 35, 9, 12, 38, 28, 27], with the property that if  $m$ ,  $n$ , and  $r$  grow proportionally, then the smallest number of measurements  $p$  for which it has been proven that algorithms recover any rank  $r$  matrix grows at most logarithmically in  $\max(m, n)$  faster than the oracle rate  $r(m + n - r)$ ; this is referred to as *near-optimal order of recoverability*. All of these algorithms are designed to return a low rank matrix that (possibly approximately) fits the measurements. Their efficacy is measured by both the computational speed of the algorithm and by when they are able to return the same answer as the minimum rank problem

$$(1.3) \quad \min_X \text{rank}(X) \quad \text{subject to} \quad \mathcal{A}(X) = b.$$

Although there are matrices for which (1.3) is NP-hard [23], there are computationally efficient algorithms which successfully solve (1.3) for many low rank matrices encountered in practice. These algorithms can generally be classified as either directly targeting the *nonconvex* problem (1.3) or solving its *convex*-relaxation, referred to as nuclear norm minimization (NNM),

$$(1.4) \quad \min_X \|X\|_* := \sum \sigma_i(X) \quad \text{subject to} \quad \mathcal{A}(X) = b,$$

in the hope that the solution of the convex-relaxation coincides with the solution of (1.3). In (1.4) the nuclear norm,  $\|X\|_*$ , is the sum of the singular values of  $X$ , denoted  $\sigma_i(X)$ . The convex-relaxation can be recast as a semidefinite program (SDP) [38] and solved using any of the algorithms designed for SDPs. Algorithms have also been designed to solve (1.4) specifically for matrix completion; these methods are primarily based on iterative soft thresholding [5, 33], where the soft thresholding operator shrinks the singular values toward zero by a specified amount, here  $\tau$ ,

$$(1.5) \quad S_\tau(X) := U\Sigma_\tau V^*, \quad \text{where} \quad \Sigma_\tau(i, i) = \max(0, \Sigma(i, i) - \tau).$$

Methods which directly approach the nonconvex objective (1.3) are typically built upon iterative hard thresholding [21, 24], where the hard thresholding operator sets all but a specified number of singular values to zero:

$$(1.6) \quad H_r(X) := U\Sigma_r V^*, \quad \text{where} \quad \Sigma_r(i, i) := \begin{cases} \Sigma(i, i), & i \leq r, \\ 0, & i > r. \end{cases}$$

Note that for both soft and hard thresholding the singular values are modified, but the singular vectors are unperturbed. Both classes of algorithms have been proven to be capable of recovering rank  $r$  matrices provided  $p \geq \text{Const } r(m+n-r) \log^\alpha(\max(m, n))$  for some  $\alpha \geq 0$ . Restricted isometry constants (RICS) can be used to establish bounds of this form but are applicable only for Gaussian sensing and provide constants,  $\text{Const}$ , of proportionality that is severely pessimistic.

**DEFINITION 1.1** (restricted isometry constants (RICs) [38]). *Let  $\mathcal{A}(\cdot)$  be a linear map of  $m \times n$  matrices to vectors of length  $p$ ,  $\mathbb{R}^{m \times n} \rightarrow \mathbb{R}^p$ , as defined in (1.1). For every integer  $1 \leq r \leq \min(m, n)$ , the RIC,  $R_r$ , of  $\mathcal{A}(\cdot)$  is defined as the smallest number such that*

$$(1.7) \quad (1 - R_r)\|X\|_F^2 \leq \|\mathcal{A}(X)\|_2^2 \leq (1 + R_r)\|X\|_F^2$$

*holds for all matrices  $X$  of rank at most  $r$ .*

More quantitative, non-RIC based, estimates have been established for the convex-relaxation (1.4) [39]. A notion of incoherence has also been employed to provide recovery guarantees [5] for entry sensing. Candès and Recht [9] have proven that with high probability, NNM (1.4) will recover the measured  $n \times n$  rank  $r$  matrix provided  $p \geq \text{Const } rn^{6/5} \log(n)$ ; later Candès and Tao [12] sharpened this result to  $p \geq \text{Const } rn \log(n)$ . Unfortunately, the incoherence approach has not given rigorous guarantees for nonconvex algorithms, which are the focus of this paper, and for this reason we will not discuss coherence further here.

The simplest hard thresholding algorithm for matrix completion is iterative hard thresholding (IHT), also called singular value projection [24],

$$(1.8) \quad X^{j+1} = H_r(X^j + \mu_j \mathcal{A}^*(b - \mathcal{A}(X^j))),$$

where the stepsize  $\mu_j$  is selected as a fixed constant (such as  $\mu_j = 0.65$  for all  $j$ ), and the adjoint of the sensing operator,  $\mathcal{A}^*(\cdot)$ , is defined as

$$(1.9) \quad \mathcal{A}^*(y) := \sum_{\ell=1}^p y(\ell) A_\ell,$$

where the  $A_\ell$  are the sensing matrices in (1.1). It has been shown in [24] that if the sensing operator  $\mathcal{A}(\cdot)$  satisfies  $R_{2r} < 1/3$ , then IHT (1.8) with constant stepsize

$\mu_j = 1/(1 + R_{2r})$  is guaranteed to recover any rank  $r$  matrix; this stepsize is selected to make the RIC based recovery condition as lax as possible and is not advocated for implementation as RICs are NP-hard to calculate [23] and hence are not available for the stepsize  $\mu_j$ . IHT has also been analyzed considering a unit stepsize [21].

IHT for matrix completion is the direct extension of IHT for compressed sensing [2], where the  $X$  is a  $k$  sparse vector of length  $N$  and the sensing operator  $\mathcal{A}(\cdot)$  is an  $n \times N$  matrix. It has been observed that IHT for compressed sensing performs dramatically better if the stepsize is selected to be optimal when the current iterate has the same support set as the sparsest solution [3]; with this stepsize selection rule the method is referred to as normalized IHT (NIHT). Here we present heuristics for the iteration dependent selection of the stepsize  $\mu_j$  in (1.8), motivated by NIHT for compressed sensing; we also refer to this best performing heuristic simply as NIHT, Algorithm 1, with its matrix completion context making clear its distinction from NIHT for compressed sensing [3].

---

**Algorithm 1.** NIHT for matrix completion.

---

**Input:**  $b = \mathcal{A}(M)$ ,  $\mathcal{A}$ ,  $r$ , and termination criteria

**Set**  $X^0 = H_r(\mathcal{A}^*(b))$ ,  $j = 0$ , and  $U_0$  as the top  $r$  left singular vectors of  $X^0$

**Repeat**

1. Set the projection operator  $P_U^j := U_j U_j^*$
2. Compute the stepsize:  $\mu_j^u = \frac{\|P_U^j \mathcal{A}^*(b - \mathcal{A}(X^j))\|_F^2}{\|\mathcal{A}(P_U^j \mathcal{A}^*(b - \mathcal{A}(X^j)))\|_2^2}$
3. Set  $X^{j+1} = H_r(X^j + \mu_j^u \mathcal{A}^*(b - \mathcal{A}(X^j)))$
4. Let  $U_{j+1}$  be the top  $r$  left singular vectors of  $X^{j+1}$
5.  $j = j + 1$

**Until** termination criteria is reached (such as  $\|b - \mathcal{A}(X^j)\|_2 \leq \text{tol}$  or  $j > \text{max iter.}$ )

**Output:**  $X^j$

---

NIHT has optimal order recovery from dense sensing, proven in section 2.2 using a standard RIC based proof reminiscent of [2, 3, 21, 24].

**THEOREM 1.2.** *Let  $\mathcal{A}(\cdot) : \mathbb{R}^{m \times n} \rightarrow \mathbb{R}^p$  have RIC  $R_{3r} < 1/5$ ; then NIHT will recover (within arbitrary precision) any rank  $r$  matrix measured by  $\mathcal{A}(\cdot)$ .*

RIC based guarantees such as Theorem 1.2 are now common for matrix completion algorithms. Unfortunately such theorems lack quantitative precision sufficient to advise a practitioner as to which of the many matrix completion algorithms to use. Much more interestingly than Theorem 1.2, we observe that NIHT is extremely efficient in a series of empirical tests; see Figures 3.3 and 3.4. For nearly all under-sampling rates  $\delta$ , NIHT is able to recover matrices of larger rank than can two of the state-of-the-art matrix completion algorithms—NNM (1.4) and PowerFactorization (PF) [22], Algorithm 2. In particular, for  $\delta \in (0.1, 1)$ , NIHT is observed to be able to recover matrices for nearly the largest achievable rank, that is,  $\rho$  near one. Note that guaranteed recovery for all rank  $r$  matrices is not possible for  $\rho > 1/2$  but that algorithms can recover most low rank matrices for  $\rho > 1/2$  [19].

Throughout this paper we will plot curves in the  $(\delta, \rho)$  plane; below a curve the associated algorithm is observed to typically recover the sensed matrix, and above the curve the algorithm is observed to typically fail to recover the sensed matrix. We refer to these curves in the  $(\delta, \rho)$  plane as phase transition curves [18]. For Gaussian sensing the phase transition for NIHT appears to oscillate with  $\rho$  between 0.85 and 0.95 independent of  $\delta$  and for entry sensing slowly varying from about  $\rho = 0.9$  at

$\delta = 0.1$  to  $\rho = 1$  at  $\delta = 1$ ; see Figure 2.2. Note that  $\rho = 1$  corresponds to achieving the oracle minimum sampling rate of  $p = r(m+n-r)$ . Moreover, for ranks where IHT (with  $\mu = 0.65$ ), NNM, and PF are also able to recover the sensed matrices, NIHT is observed to be faster for entry sensing and typically faster for Gaussian sensing (1.1); see Figures 3.5 and 3.6.

The manuscript is organized as follows. In section 2 we derive and discuss the theory and practice of NIHT, contrasting the stepsize heuristic with constant stepsize IHT. In section 3 we present detailed numerical comparisons of NIHT with NNM (1.4) and PF, Algorithm 2.

**2. Normalized iterative hard thresholding (NIHT).** Iterative algorithms for matrix completion are often designed by successively updating a current estimate  $X^j$  in order to decrease a measurement fidelity objective, such as

$$\|b - \mathcal{A}(X^j)\|_2^2.$$

This is typically achieved by modifying  $X^j$  along the objective's negative gradient

$$2\mathcal{A}^*(b - \mathcal{A}(X^j)).$$

For example, basic gradient descent is given by

$$X^j + \mu_j \mathcal{A}^*(b - \mathcal{A}(X^j)),$$

where the stepsize  $\mu_j$  is typically selected to ensure a decrease in the objective in each iteration. This approach can also be employed for constrained problems such as (1.3) by using alternate projection between a steepest descent update and a projection back onto the space of rank  $r$  matrices; for a more general discussion of alternating projection methods, see [31]. IHT (1.8) is a particularly simple example of such an alternating projection method [21, 24]. Many, though not all, of the matrix completion algorithms are more involved variants of projected descent methods, such as modifying the descent direction to ensure the update remains on the manifold of rank  $r$  matrices [43, 44, 40, 35], using iterative soft thresholding (1.5) possibly with modified search directions to solve (1.4) or a variant thereof [21, 5, 6, 41, 33, 25, 26, 32], and multistage variants [15, 30, 45] reminiscent of the compressed sensing algorithms CoSaMP [37] and subspace pursuit [14]. For a recent review and empirical comparison of many of these algorithms, see [36].

The effectiveness of IHT is determined by the selection of the stepsize  $\mu_j$ . Selecting  $\mu_j$  too small both causes the algorithm to be slow and encourages convergence to local rather than the global minima, whereas selecting  $\mu_j$  too large can result in lack of convergence. This issue has been widely discussed in the field of nonlinear optimization, including for the matrix completion algorithms discussed in [43, 44, 21, 40, 35], which draw from the nonlinear optimization literature. Here we consider an alternative motivation drawn from compressed sensing. Large-scale empirical testing [34] of a fixed stepsize for IHT in compressed sensing suggested  $\mu_j = 0.65$ , and we find this to also be an effective choice for a fixed stepsize for the matrix completion variant of IHT (1.8); see Figures 3.1 and 3.2. Even more effective than the constant stepsize  $\mu_j = 0.65$  is the adaptive stepsize of NIHT [3].

Compressed sensing and sparse approximation algorithms seek a (possibly approximate) solution to an underdetermined system of equations  $b = Ax$  with fewer nonzeros than the number of rows in  $A$ . The prototypical sparse approximation algorithm is

$$(2.1) \quad \min_x \|x\|_0 \text{ subject to } b = Ax,$$

where  $\|x\|_0$  counts the number of nonzeros in  $x$ . As with (1.3), there are  $A$  for which solving (2.1) is NP-hard [23]. The complication in solving (2.1) is the identification of the support set of the sparsest vector; once the support set is identified, it is easy to solve for the nonzero coefficients by solving the resulting overdetermined system of equations. IHT for compressed sensing is analogous to (1.8),

$$x^{j+1} = HT_k(x^j + \mu_j A^*(b - Ax^j)),$$

but with  $HT_k(\cdot)$  setting all but the  $k$  largest (in magnitude) entries of the vector to zero and  $A^*$  denoting the complex conjugate of  $A$ . NIHT for compressed sensing corresponds to selecting the  $\mu_j$  to be the optimal stepsize provided  $x^j$  has identified the support set of the solution to (2.1); the stepsize is given by

$$\mu_j := \frac{\|A_{\Lambda^j}^*(b - Ax^j)\|_2^2}{\|A_{\Lambda^j} A_{\Lambda^j}^*(b - Ax^j)\|_2^2},$$

where  $A_{\Lambda^j}$  is the restriction of  $A$  to the columns corresponding to the nonzeros in  $x^j$ . NIHT for matrix completion, Algorithm 1, is similarly motivated.

When IHT is converging to the minimal rank solution, each of the singular vectors and values of the current estimate  $X^j$  must also be converging to the singular vectors and values of the minimum rank solution. Proximity to the correct singular vectors motivates selecting the stepsize as if the singular vectors had been correctly identified and the update is being used to improve the singular values. Let the iterate  $X^j$  be of rank  $r$  with the SVD  $X^j = U_j \Sigma_j V_j^*$ ; then we denote the projection onto the top  $r$  left and right singular vector spaces as

$$(2.2) \quad P_U^j := U_j U_j^*$$

and

$$(2.3) \quad P_V^j := V_j V_j^*,$$

respectively. A search direction can be projected to the span of the singular vectors by applying (2.2) from the left and (2.3) from the right, for instance, the projected negative gradient descent direction is given by  $W_j^{uv} := P_U^j \mathcal{A}^*(b - \mathcal{A}(X^j)) P_V^j$ . Alternatively, a search direction can be projected to the span of just the left or right singular by applying only (2.2) from the left or (2.3) from the right, respectively, with search directions given by  $W_j^u := P_U^j \mathcal{A}^*(b - \mathcal{A}(X^j))$  and  $W_j^v := \mathcal{A}^*(b - \mathcal{A}(X^j)) P_V^j$ . Using any of these restricted search directions to update the current iterate  $X^j$  results in the next iterate also being restricted to the same projected spaces, which would not allow the iterates to converge to the lowest rank solution unless the projected directions had been exactly correctly identified. The analogue in compressed sensing would be to update only the support set of the past iterate. Although the projected directions should not be used as the update direction, they provide useful information for selecting the stepsize.

The three above-mentioned projected directions motivate the three stepsizes

$$(2.4) \quad \mu_j^u := \frac{\|P_U^j \mathcal{A}^*(b - \mathcal{A}(X^j))\|_F^2}{\|\mathcal{A}(P_U^j \mathcal{A}^*(b - \mathcal{A}(X^j)))\|_2^2},$$

$$(2.5) \quad \mu_j^v := \frac{\|\mathcal{A}^*(b - \mathcal{A}(X^j)) P_V^j\|_F^2}{\|\mathcal{A}(\mathcal{A}^*(b - \mathcal{A}(X^j)) P_V^j)\|_2^2},$$

$$(2.6) \quad \mu_j^{uv} := \frac{\|P_U^j \mathcal{A}^*(b - \mathcal{A}(X^j)) P_V^j\|_F^2}{\|\mathcal{A}(P_U^j \mathcal{A}^*(b - \mathcal{A}(X^j)) P_V^j)\|_2^2}$$

and three associated variants of NIHT, each of which use the same unrestricted negative gradient search direction (1.8), but with three different stepsize heuristics (2.4), (2.5), and (2.6). We refer to the three variants of NIHT associated with these stepsizes as NIHT when using (2.4), NIHT with row restriction when using (2.5), and NIHT with column and row restriction when using (2.6). NIHT is observed to have the best empirical performance (see section 3), motivating its abridged name. NIHT is stated in greater detail in Algorithm 1. Following the submission of this manuscript the authors were alerted to [28], which proposes an algorithm for matrix completion similar to NIHT in its use of linesearch stepsize based on projection to the subspace of the top singular vectors of its current iterate.

Although NIHT has much in common with the Riemannian optimization methods of [43, 44], NIHT lacks the safeguards and sophistication of such nonconvex optimization algorithms. In particular, Algorithm 1 lacks a safeguard to ensure a decrease in  $\|b - \mathcal{A}(X^j)\|_2$  at each step. However, each of the stepsizes in (2.4)–(2.6) are bounded above and below for sensing operators  $\mathcal{A}(\cdot)$  with bounded RICs (1.7) and can be proven to converge when the sensing operator's RICs are sufficiently small; see Theorem 1.2. Note that a similar stepsize calculation lacking the projection to rank  $r$  matrices would result in possibly unbounded stepsizes.

**2.1. NIHT empirical average case behavior.** We observe NIHT, Algorithm 1, to typically be able to recover the same or larger rank than IHT can with a well-chosen fixed stepsize ( $\mu_j = 0.65$ ), and that NIHT converges faster than IHT. We evaluate NIHT's ability to recover  $m \times n$  matrices with rank  $r$  from  $p$  measurements (1.1), from both entry measurements drawn uniformly at random and dense measurements where each of the  $p$  sensing matrices  $A_\ell$  are drawn independent and identically distributed (i.i.d.) Gaussian  $\mathcal{N}(0, 1/\sqrt{mn})$ . Tests are conducted for measured  $m \times n$  matrices of rank  $r$  drawn from two models: the Gaussian model [38], where the measured matrix is constructed as  $X_0 = CD$  with  $C$  and  $D$  being  $m \times r$  and  $r \times n$  matrices with entries drawn i.i.d. Gaussian  $\mathcal{N}(0, 1)$ , and the “equalized Gaussian model,” where the measured matrix is constructed as  $X_0 = UI_rV^*$  with  $I_r$  being the  $r \times r$  identity matrix and  $U$  and  $V$  being  $m \times r$  and  $n \times r$  matrices drawn uniformly at random from the Grassmannian manifold of matrices with orthonormal columns. The recovery properties of NIHT are observed to be the same for both of these models. We present results only for the Gaussian model.

Without loss of generality, we order  $m$  and  $n$  with  $m \leq n$  and define their ratio as

$$(2.7) \quad \gamma := \frac{m}{n}.$$

For each value of  $n$  tested, we conduct tests for  $m$  such that  $\gamma = 1/4, 1/2, 3/4$ , and 1. For each  $m, n$  pair we conduct tests with the number of measurements being  $p = mn(j/10)$  for  $j = 1, 2, \dots, 10$ , which corresponds to  $\delta = j/10$  for the same values of  $j$ . The reconstruction algorithms are substantially faster for entry measurements, as dense measurements have an additional requirement of  $pmn$  scalar multiplications for the application of  $\mathcal{A}(\cdot)$ , which scales proportionally to  $n^4$  in our testing environment. For this reason the tests for dense Gaussian sensing are conducted for  $n = 40$  and  $n = 80$ , whereas the tests for entry sensing are conducted for  $n = 40, 80, 160, 200, 400$ , and 800. We consider an algorithm to have successfully recovered<sup>1</sup> the sensed rank  $r$

<sup>1</sup>Greater accuracy conditions were tested for a subset of problems. In each instance it was observed that recovery within arbitrary precision was possible once a matrix was identified to within a  $2 \times 10^{-3}$  relative error in the Frobenius norm.

matrix  $X_0$  if it returns a rank  $r$  matrix  $X^{output}$  that is within  $2 \times 10^{-3}$  of the sensed matrix in the relative Frobenius norm,  $\|X^{output} - X_0\|_F \leq 2 \times 10^{-3} \|X_0\|_F$ . For each triple  $m, n, p$  we select a value of  $r$  sufficiently small that the algorithm *successfully recovers the sensed matrix in each of ten randomly drawn tests*; we then increase the rank of the sensed matrices, conducting ten tests per rank, until the rank is sufficiently large that the algorithm *fails to recover the sense matrix in each of ten randomly drawn tests*. We refer to the largest value of  $r$  for which the algorithm succeeded in each of ten tests as  $r_{min}$  and the smallest value of  $r$  for which the algorithm failed in each of the ten tests at  $r_{max}$ . NIHT and IHT terminate if  $\|b - \mathcal{A}(X^j)\|_2 / \|b\|_2 < 10^{-5}$  or if the multiplicative average of the last fifteen linear convergence rates are greater than  $\kappa$ ,

$$(2.8) \quad \left( \frac{\|b - \mathcal{A}(X^{j+15})\|_2}{\|b - \mathcal{A}(X^j)\|_2} \right)^{1/15} > \kappa.$$

Unless otherwise stated we set  $\kappa = 0.999$ .

The values of  $r_{min}$  and  $r_{max}$  for NIHT are displayed in Figure 2.1 for Gaussian sensing with  $n = 80$  (left panel) and for entry sensing with  $n = 800$  (right panel). The same data is displayed in Figure 2.2, but with the vertical axis being the values of  $\rho$  calculated from  $(r_{min} + r_{max})/2$ . The exact values of  $r_{min}$ ,  $r_{max}$  and associated  $\rho_{min}$ ,  $\rho_{max}$  calculated from (1.2) for these, as well as smaller  $n$ , are listed in Tables 2.1 and 2.2 for Gaussian sensing and entry sensing, respectively.

The remarkable effectiveness of NIHT is evident in Figure 2.2 through the approximate phase transition, calculated using  $(r_{min} + r_{max})/2$ . Though the phase transition for Gaussian sensing displayed in Figure 2.2 (left panel) appears erratic due to the small value of  $n = 80$  and associated large changes in  $\rho$  for a rank one change, it is surprising that the phase transitions remain between 0.85 and 0.95 for each of  $\gamma = 1, 3/4, 1/2$ , and  $1/4$ , as well as for each of  $\delta = j/10$  for  $j = 1, 2, \dots, 10$ . The phase transition occurring between 0.85 and 0.95 indicates that, irrespective of the degree of undersampling,  $\delta$ , NIHT is able to recover rank  $r$  matrices for the number of measurements being a small multiple of the minimum number; that is,  $p = \text{Const} \cdot r(m + n - r)$  for  $\text{Const} < 1.2$ . NIHT exhibits a similarly high phase transition for entry sensing in Figure 2.2 (right panel). The entry sensing tests for the larger value of  $n = 800$  greatly reduces the sensitivity of  $\rho$  to small changes in  $r$ , resulting in much smoother observed phase transitions. For  $\gamma = 1, 3/4$ , and  $1/2$  we observe phase transitions that slowly increase from approximately  $\rho = 0.9$  to 1 as  $\delta$  increases from 0.2 to 1. The smaller value of  $\gamma = 1/4$  shows substantially reduced phase transitions for entry sensing, but in section 3 we will observe that even this lower phase transition compares favorably to other matrix completion algorithms. The data in Table 2.1 for  $m = n$  and  $p = mn/10$  suggest that the lower phase transition for  $\delta = 1/10$  may be an artifact of the small problem sizes. Similarly, we observe that increasing the problem size from  $n = 80$  to 800 results in substantial increases in the phase transitions shown in Figure 3.2, including that for  $\gamma = 1/4$ .

The convergence rate stopping criteria (2.8) plays an important role in achieving the observed high phase transitions; setting  $\kappa$  to the very slow 0.995 is observed to noticeably reduce the largest recoverable rank as compared to the seemingly impractically slow  $\kappa = 0.999$ . Figure 3.1 shows the increase in the phase transitions when  $\kappa$  is increased from 0.995 (blue) to 0.999 (black). Figure 2.3 shows that this increase in  $\kappa$  allows for some of the tests that terminate with error greater than  $2 \times 10^{-3}$  to further iterate and decrease the error sufficiently for the relative error stopping criteria  $\|b - \mathcal{A}(X^j)\|_2 / \|b\|_2 < 10^{-5}$  to be active. Raising in the phase transition by



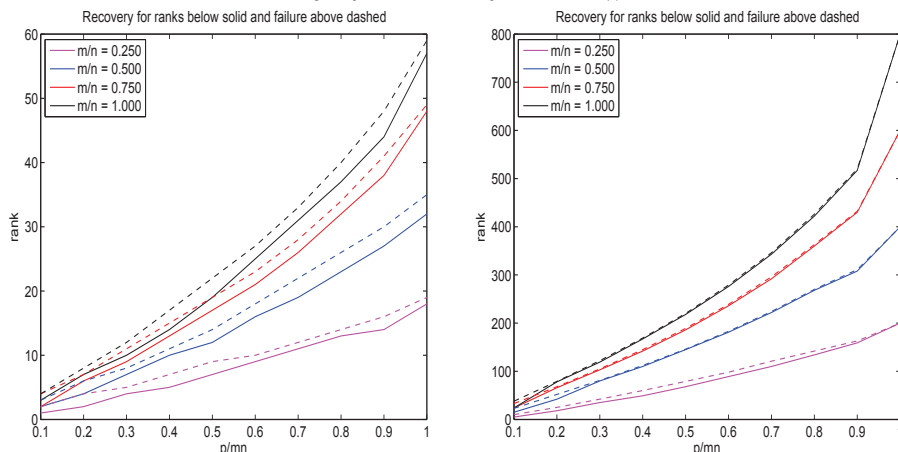


FIG. 2.1. For each rank above the dashed lines NIHT failed to recover the sensed matrix in each of ten randomly drawn tests per rank, whereas for each rank below the solid lines NIHT succeeded in recovering the sensed matrix in each of ten randomly drawn tests per rank. The vertical axis is the rank of the sensed matrix, and the horizontal axis is the undersampling ratio  $\delta$ . Left panel: Gaussian sensing with  $n = 80$ . Right panel: Entry sensing with  $n = 800$ .

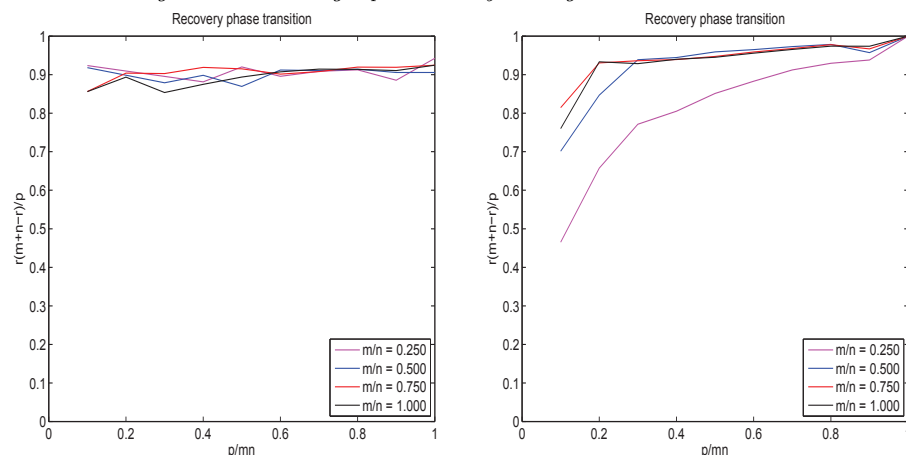


FIG. 2.2. Phase transition of NIHT with horizontal axis  $\delta$  and vertical axis  $\rho$ , where  $\rho$  is calculated using the average of  $r_{\min}$  and  $r_{\max}$  from Tables 2.1 and 2.2. Left panel: Gaussian sensing with  $n = 80$ . Right panel: Entry sensing with  $n = 800$ .

increasing  $\kappa$  comes at the cost of the maximum number of iterations increasing from approximately 1500 to 6500 and the associated time to completion. Although this nearly fourfold increase in the time to completion may seem inadvisable, no other algorithm is observed to be able to recover low rank matrices for such large ranks. The other algorithms tested are unable to increase the recoverable rank by extending the stopping criteria; see, for instance, the right panel of Figure 2.3, where PF is observed to have clear separation between problem instances where the algorithm converges to the sensed matrix and when it returns a low rank matrix that differs substantially from the measured matrix.

**2.2. Proof of Theorem 1.2.** This proof of Theorem 1.2 is similar to those in [2, 3, 21, 24], differing only in how the stepsize  $\mu_j^u$  is bounded, and is equally valid for each of the three variants of NIHT using the stepsizes (2.4)–(2.5). The proof follows by first deriving an inequality where  $\|X^{j+1} - X_0\|_F$  is bounded by a factor multiplying

TABLE 2.1

For each listed  $m, n, p$  triple, NIHT with  $p$  Gaussian measurements is tested for ten randomly drawn  $m \times n$  rank  $r$  matrices per rank and is observed to recover each of the ten measured matrices for all  $r \leq r_{\min}$  and to fail to recover each of the ten measured matrices per rank for  $r \geq r_{\max}$ .

NIHT with Gaussian measurements													
$m$	$n$	$p$	$r_{\min}$	$r_{\max}$	$\rho_{\min}$	$\rho_{\max}$	$m$	$n$	$p$	$r_{\min}$	$r_{\max}$	$\rho_{\min}$	$\rho_{\max}$
10	40	40	0	0	0.000	0.000	20	80	160	1	2	0.619	1.225
		80	1	2	0.613	1.200			320	2	4	0.613	1.200
		120	2	3	0.800	1.175			480	4	5	0.800	0.990
		160	2	4	0.600	1.150			640	5	7	0.742	1.017
		200	3	5	0.705	1.125			800	7	9	0.814	1.024
		240	4	5	0.767	0.938			960	9	10	0.853	0.938
		280	5	7	0.804	1.075			1120	11	12	0.874	0.943
		320	6	7	0.825	0.941			1280	13	14	0.884	0.941
		360	7	9	0.836	1.025			1440	14	16	0.836	0.933
		400	8	10	0.840	1.000			1600	18	19	0.922	0.962
20	40	80	1	2	0.738	1.450	40	80	320	2	3	0.738	1.097
		160	2	3	0.725	1.069			640	4	6	0.725	1.069
		240	3	5	0.713	1.146			960	7	8	0.824	0.933
		320	4	6	0.700	1.012			1280	10	11	0.859	0.937
		400	6	7	0.810	0.927			1600	12	14	0.810	0.927
		480	8	9	0.867	0.956			1920	16	18	0.867	0.956
		560	9	11	0.820	0.963			2240	19	22	0.857	0.963
		640	11	13	0.842	0.955			2560	23	26	0.871	0.955
		720	13	15	0.849	0.938			2880	27	30	0.872	0.938
		800	16	18	0.880	0.945			3200	32	35	0.880	0.930
30	40	120	1	2	0.575	1.133	60	80	480	2	4	0.575	1.133
		240	3	4	0.838	1.100			960	6	7	0.838	0.970
		360	4	6	0.733	1.067			1440	9	11	0.819	0.985
		480	6	8	0.800	1.033			1920	13	15	0.860	0.977
		600	7	10	0.735	1.000			2400	17	19	0.871	0.958
		720	11	12	0.901	0.967			2880	21	23	0.868	0.934
		840	12	15	0.829	0.982			3360	26	28	0.882	0.933
		960	15	17	0.859	0.939			3840	32	34	0.900	0.939
		1080	18	21	0.867	0.953			4320	38	41	0.897	0.940
		1200	23	25	0.901	0.938			4800	48	49	0.920	0.929
40	40	160	1	2	0.494	0.975	80	80	640	3	4	0.736	0.975
		320	3	4	0.722	0.950			1280	7	8	0.837	0.950
		480	5	7	0.781	1.065			1920	10	12	0.781	0.925
		640	7	9	0.798	0.998			2560	14	17	0.798	0.950
		800	9	11	0.799	0.949			3200	19	22	0.837	0.949
		960	12	14	0.850	0.963			3840	25	27	0.879	0.935
		1120	15	17	0.871	0.956			4480	31	33	0.893	0.935
		1280	18	20	0.872	0.938			5120	37	40	0.889	0.938
		1440	21	24	0.860	0.933			5760	44	48	0.886	0.933
		1600	28	30	0.910	0.938			6400	57	59	0.917	0.931

$\|X^j - X_0\|_F$  and then showing that this multiplicative factor is less than one when the theorem's condition that the sensing operator has RIC  $R_{3r} < 1/5$  is satisfied. Let  $X_0$  be the measured rank  $r$  matrix with measurements  $b = \mathcal{A}(X_0)$ , and let

$$W^j = X^j + \mu_j^u \mathcal{A}^*(b - \mathcal{A}(X^j))$$

be the intermediate update to  $X^j$  in NIHT, as stated in Algorithm 1, before it is projected to the rank  $r$  update  $X^{j+1}$ . The Eckart–Young theorem ensures that  $X^{j+1}$  is the rank  $r$  matrix nearest to  $W^j$  in the Frobenius norm,

$$(2.9) \quad \|W^j - X^{j+1}\|_F^2 \leq \|W^j - X_0\|_F^2.$$

TABLE 2.2  
 For each listed  $m, n, p$  triple, NIHT with  $p$  entry measurements is tested for ten randomly drawn  $m \times n$  rank  $r$  matrices per rank and is observed to recover each of the ten measured matrices for all  $r \leq r_{min}$  and to fail to recover each of the ten measured matrices per rank for  $r \geq r_{max}$ .

NIHT with entry measurements									
$m$	$n$	$p$	$r_{min}$	$r_{max}$	$\rho_{min}$	$\rho_{max}$	$m$	$n$	$p$
50	200	1000	0	2	0.000	0.496	100	400	4000
		2000	1	5	0.124	0.613			8000
		3000	3	9	0.247	0.723			12000
		4000	6	14	0.366	0.826			16000
		5000	10	19	0.480	0.878			20000
		6000	16	23	0.624	0.970			24000
		7000	20	29	0.657	0.916			28000
		8000	27	34	0.753	0.918			32000
		9000	34	39	0.816	0.914			36000
		10000	50	50	1.000	1.000			40000
100	200	2000	1	5	0.149	0.738	200	400	8000
		4000	6	12	0.441	0.864			16000
		6000	12	19	0.576	0.890			24000
		8000	22	28	0.764	0.952			32000
		10000	28	36	0.762	0.950			40000
		12000	38	46	0.830	0.974			48000
		14000	51	56	0.907	0.976			56000
		16000	59	67	0.889	0.976			64000
		18000	71	75	0.903	0.938			72000
		20000	100	100	1.000	1.000			80000
150	200	3000	2	8	0.232	0.912	300	400	12000
		6000	11	17	0.622	0.944			24000
		9000	22	26	0.802	0.936			36000
		12000	32	37	0.848	0.965			48000
		15000	45	48	0.915	0.966			60000
		18000	57	56	0.928	0.967			72000
		21000	71	75	0.943	0.982			84000
		24000	84	91	0.931	0.982			96000
		27000	99	103	0.920	0.942			108000
		30000	150	150	1.000	1.000			120000
200	200	4000	1	9	0.100	0.880	400	800	16000
		8000	9	20	0.440	0.950			32000
		12000	27	31	0.839	0.953			48000
		16000	39	43	0.880	0.963			64000
		20000	52	56	0.905	0.963			80000
		24000	66	71	0.918	0.973			96000
		28000	84	88	0.948	0.981			112000
		32000	101	107	0.944	0.980			128000
		36000	119	124	0.929	0.951			144000
		40000	200	200	1.000	1.000			160000

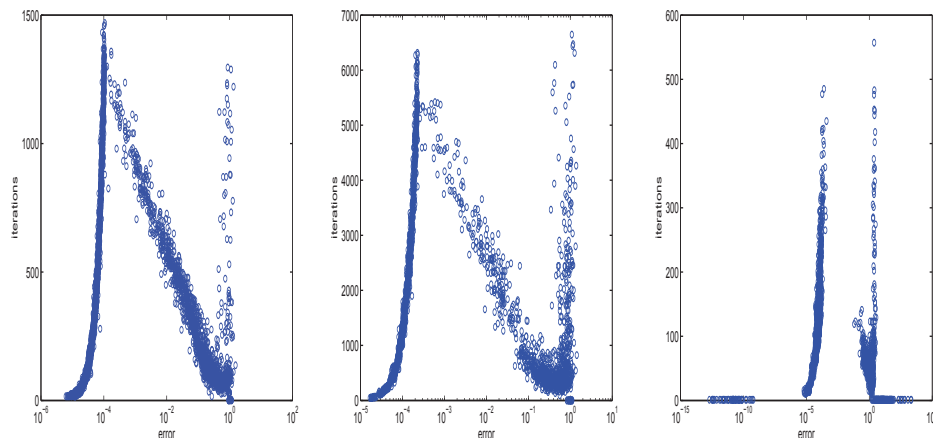


FIG. 2.3. Iteration versus error for NIHT with Gaussian sensing using convergence rate stopping criteria 0.995 and 0.999 in the left and middle panels, respectively, and for PF [22] in the right panel. The plots include the results for each of the tests conducted for  $n = 40$  and  $80$ , comprising 20,640 tests in the left panel, 5,000 tests in the middle panel, and 4,410 tests in the right panel.

Expanding  $\|W^j - X^{j+1}\|_F^2$  and bounding it from above using (2.9) gives

$$\begin{aligned} \|W^j - X^{j+1}\|_F^2 &= \|W^j - X_0 + X_0 - X^{j+1}\|_F^2 \\ &= \|W^j - X_0\|_F^2 + \|X_0 - X^{j+1}\|_F^2 \\ &\quad + 2\langle W^j - X_0, X_0 - X^{j+1} \rangle \\ &\leq \|W^j - X_0\|_F^2. \end{aligned}$$

Canceling  $\|W^j - X_0\|_F^2$  in the above inequality gives the inequality

(2.10)

$$\begin{aligned} \|X^{j+1} - X_0\|_F^2 &\leq 2\langle W^j - X_0, X^{j+1} - X_0 \rangle \\ &= 2\langle X^j - X_0, X^{j+1} - X_0 \rangle - 2\mu_j^u \langle \mathcal{A}^* \mathcal{A}(X^j - X_0), X^{j+1} - X_0 \rangle \\ &= 2\langle X^j - X_0, X^{j+1} - X_0 \rangle - 2\mu_j^u \langle \mathcal{A}(X^j - X_0), \mathcal{A}(X^{j+1} - X_0) \rangle. \end{aligned}$$

Let  $Q_j \in \mathbb{R}^{m \times 3r}$  have orthonormal columns which span the space of all of the columns of  $X_0$ ,  $X^j$ , and  $X^{j+1}$ , and let  $P_Q^j := Q_j Q_j^*$  be the projection operator to this column space; in particular,  $P_Q^j X_0 = X_0$ ,  $P_Q^j X^j = X^j$ , and  $P_Q^j X^{j+1} = X^{j+1}$ . Define  $\mathcal{A}_Q(Z) := \mathcal{A}(P_Q^j Z)$ , which corresponds to replacing the sensing matrices  $\{A_\ell\}_{\ell=1}^p$  of the unrestricted sensing operator  $\mathcal{A}(\cdot)$  with the sensing matrices  $\{P_Q^j A_\ell\}_{\ell=1}^p$  and the correspondingly associated adjoint operator  $\mathcal{A}_Q^*(\cdot)$  as would follow in the definition (1.9) with  $A_\ell$  replaced with  $P_Q^j A_\ell$ . With these projected operators we can express and further bound the inequality (2.11) as follows:

$$\begin{aligned} \|X^{j+1} - X_0\|_F^2 &\leq 2\langle X^j - X_0, X^{j+1} - X_0 \rangle - 2\mu_j^u \langle \mathcal{A}(X^j - X_0), \mathcal{A}(X^{j+1} - X_0) \rangle \\ &= 2\langle X^j - X_0, X^{j+1} - X_0 \rangle - 2\mu_j^u \langle \mathcal{A}_Q(X^j - X_0), \mathcal{A}_Q(X^{j+1} - X_0) \rangle \\ &= 2\langle X^j - X_0, (X^{j+1} - X_0) - \mu_j^u \mathcal{A}_Q^*(\mathcal{A}_Q(X^{j+1} - X_0)) \rangle \\ &= 2\langle X^j - X_0, (I - \mu_j^u \mathcal{A}_Q^*(\mathcal{A}_Q))(X^{j+1} - X_0) \rangle \\ &\leq 2\|I - \mu_j^u \mathcal{A}_Q^* \mathcal{A}_Q\|_2 \cdot \|X^j - X_0\|_F \cdot \|X^{j+1} - X_0\|_F. \end{aligned}$$

Canceling one power of  $\|X^{j+1} - X_0\|_F$  from each side of the last inequality gives the desired bound on the error at step  $j + 1$  as compared to the error at step  $j$ ,

$$(2.11) \quad \|X^{j+1} - X_0\|_F \leq 2\|I - \mu_j^u \mathcal{A}_Q^* \mathcal{A}_Q\|_2 \cdot \|X^j - X_0\|_F,$$

and it remains only to bound the operator norm  $\|I - \mu_j^u \mathcal{A}_Q^* \mathcal{A}_Q\|_2$ .

The operator  $\mathcal{A}_Q^* \mathcal{A}_Q(\cdot)$  is self-adjoint and acts on the projected space of rank  $3r$  matrices defined by  $P_Q^j$ ; as such, its spectrum satisfies the RIC bounds

$$(2.12) \quad 1 - R_{3r} \leq \lambda(\mathcal{A}_Q^* \mathcal{A}_Q) \leq 1 + R_{3r}.$$

Similarly, the inverse of the stepsize  $\mu_j^u$  is the ratio of the operator  $\mathcal{A}(\cdot)$  acting on a rank  $r$  matrix in the space defined by  $P_U^j$ , giving the RIC based bounds

$$(2.13) \quad \frac{1}{1 + R_r} \leq \mu_j^u = \frac{\|P_U^j \mathcal{A}^*(b - \mathcal{A}(X^j))\|_F^2}{\|\mathcal{A}(P_U^j \mathcal{A}^*(b - \mathcal{A}(X^j)))\|_2^2} \leq \frac{1}{1 - R_r}.$$

Combining the bounds on the spectrum of  $\mathcal{A}_Q^* \mathcal{A}_Q$  in (2.12) and the stepsize in (2.13), we bound the spectrum of  $I - \mu_j^u \mathcal{A}_Q^* \mathcal{A}_Q$  as

$$1 - \frac{1 + R_{3r}}{1 - R_r} \leq \lambda(I - \mu_j^u \mathcal{A}_Q^* \mathcal{A}_Q) \leq 1 - \frac{1 - R_{3r}}{1 + R_r}.$$

The magnitude of the lower bound above is greater than that of the upper bound, giving the operator bound

$$(2.14) \quad \|I - \mu_j^u \mathcal{A}_Q^* \mathcal{A}_Q\|_2 \leq \frac{1 + R_{3r}}{1 - R_r} - 1,$$

which is strictly less than  $1/2$  due to the condition of the theorem  $R_{3r} < 1/5$ . Consequently, the bound (2.11) results in a strict linear decrease in the error  $\|X^j - X_0\|_F$  at each iteration, proving the convergence of  $X^j$  to  $X_0$ .

**3. Comparison with other algorithms.** Matrix completion is a rapidly evolving field with numerous algorithms introduced in the last few years [21, 24, 22, 43, 44, 40, 5, 6, 41, 15, 33, 25, 26, 30, 45, 32, 35, 9, 12, 38]. A recent review of matrix completion algorithms, including most of the aforementioned, is presented in [36] along with extensive numerical comparisons. The focus of the numerical tests presented here is on quantifying the largest possible rank recoverable for an algorithm as a function of  $p/mn$  and exploring whether this phase transition is stable as the matrix size increases. This testing environment probes algorithms in the region where their convergence rates slow, causing the tests to have an unusually high computational burden. The tests presented in this paper required 4.67 CPU years<sup>2</sup> run on hex core Intel X5650 CPUs with 24 GB of RAM.

The empirical behavior of NIHT has been presented in section 2.1. Here we contrast the performance of NIHT with fixed stepsize IHT ( $\mu_j = 0.65$ ), NNM using a semidefinite programming formulation [38] and the software package SDPT3 [42], and PF [22], Algorithm 2. These three algorithms are selected as representative examples of hard thresholding algorithms, IHT, convex relaxations, NNM, and a quite distinct

<sup>2</sup>All algorithms were written using MATLAB R2011b with the default SVD, as opposed to the potentially faster PROPACK [29].

variant of optimization on the manifold of low rank matrices, PF. PF was selected due to both its simplicity and its remarkably high phase transition [22]. The primary focus of this comparison is to determine the largest rank recoverable by an algorithm for a given  $m, n, p$  triple. Timings are included for completeness. Each algorithm is tested as described in the first paragraph of section 2.1.

---

**Algorithm 2.** PowerFactorization (PF) for matrix completion.

---

**Input:**  $U^0 \in \mathbb{R}^{m \times r}$ ,  $V^0 \in \mathbb{R}^{r \times n}$

**Repeat**

1. Hold  $V^{j-1}$  fixed, solve  $U^j = \arg \min_U \|\mathcal{A}(UV^{j-1}) - b\|_2$
2. Hold  $U^j$  fixed, solve  $V^j = \arg \min_V \|\mathcal{A}(U^jV) - b\|_2$
3.  $j = j + 1$

**Until** some criteria meets

**Output**  $X^j = U^jV^j$

---

**3.1. Comparison of IHT and NIHT.** We consider (1.8) with four stepsize choices—IHT with fixed stepsize  $\mu_j = 0.65$  as well as three variants of NIHT with iteration adaptive stepsizes as stated in (2.4)–(2.6). The RIC based analysis of NIHT with stepsize (2.4) presented in section 2.2 is equally valid for stepsizes (2.5) and (2.6). Unfortunately, this worst case analysis gives little indication of their average case effectiveness. Tests were conducted for matrices with aspect ratio  $m/n = 1, 3/4, 1/2, 1/4$ , and  $1/8$  for  $n = 40$  and  $n = 80$ . The variant with stepsize (2.5) was able to recover matrices of the same rank as (2.4) when  $m/n = 1, 3/4$ , and  $1/2$ , but was able to recover only substantially lower rank matrices for the more rectangular aspect ratios  $m/n = 1/4$  and  $1/8$ . The NIHT variant with stepsize (2.6) was able to recover only matrices of greatly reduced rank as compared to (2.4) and (2.5). For conciseness we limit ourselves to presenting only the results for the adaptive stepsize variant (2.4), which we refer to simply as NIHT and state in greater detail as Algorithm 1.

Figures 3.1 and 3.2 display the estimated phase transition with  $\rho$  calculated using the average of  $r_{min}$  and  $r_{max}$  as described in section 2.1. Figure 3.1 displays the phase transition with Gaussian sensing for NIHT with stopping criteria  $\kappa = 0.999$  (black) and  $0.995$  (blue) as well as IHT with fixed stepsize  $\mu_j = 0.65$  (red) with  $\kappa = 0.999$ . Increasing  $\kappa$  is observed to substantially increase the recoverable rank. For the same stopping criteria, NIHT is observed to recover rank  $r$  matrices for  $r$  at least as high as IHT. The average timings for the associated tests with  $\kappa = 0.999$  and  $m = n = 40$  are displayed in Figure 3.5 (b) and (d) for NIHT and IHT, respectively, and the ratio of their average timings is displayed in Figure 3.6 (b). NIHT is observed to be faster than IHT except for the region of large  $\delta$  and  $\rho$ , where IHT is beginning to fail to recover the solution to (1.3) but NIHT remains able to recover the solution to (1.3).

Figure 3.2 displays the phase transition for entry sensing (1.1) and NIHT with  $n = 800$  (blue) and  $n = 80$  (black) as well as IHT with stepsize  $\mu_j = 0.65$  and  $n = 80$  (red). NIHT and IHT are observed to be able to recover rank  $r$  matrices for nearly the same rank with  $n = 80$ . Increasing the matrix size from  $n = 80$  to  $n = 800$  results in a dramatic increase in the phase transitions, with each curve surprisingly close to the maximum achievable  $\rho = 1$ . All entry sensing tests use stopping criteria  $\kappa = 0.999$ . The average timings for the associated tests with  $n = m = 80$  are displayed in Figure 3.5 (a) and (c) for NIHT and IHT, respectively, and the ratio of their average timings is displayed in Figure 3.6 (a). NIHT is observed to always be faster than IHT, typically taking just under half the time.

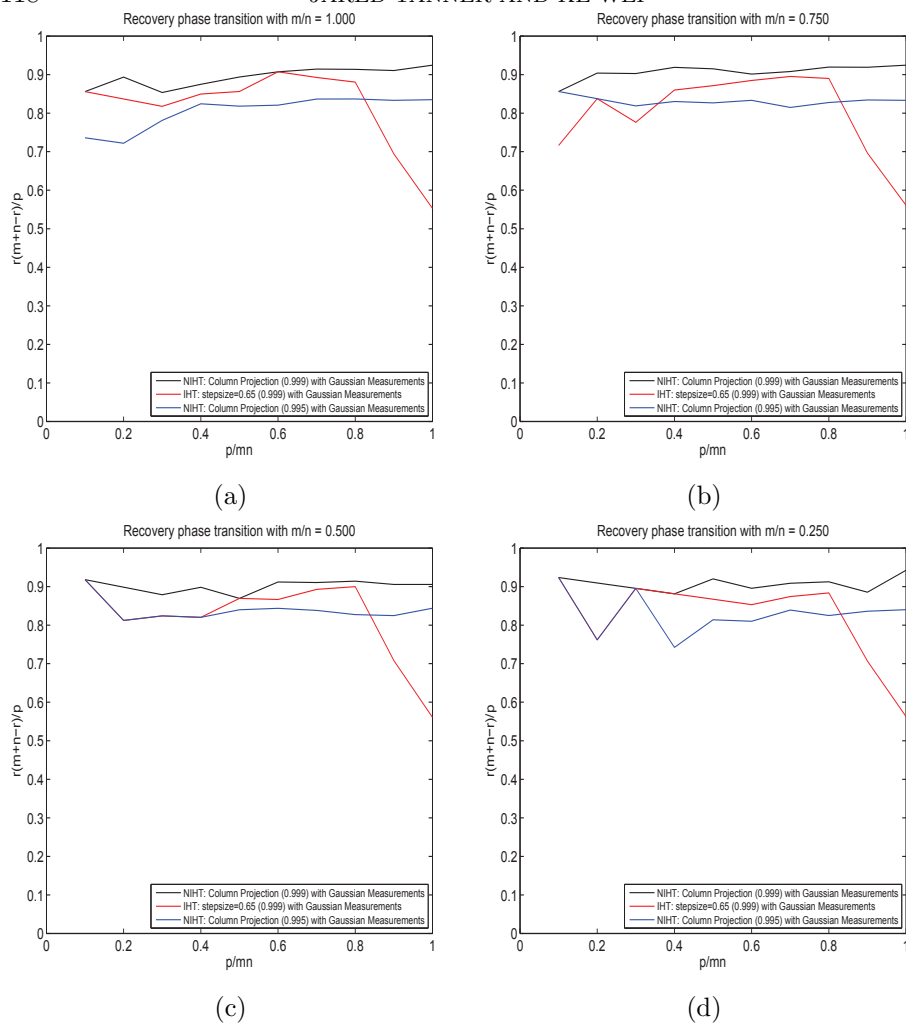


FIG. 3.1. Phase transition for Gaussian sensing and algorithms: NIHT with stopping criteria  $\kappa = 0.999$  and  $\kappa = 0.995$  as well as IHT with stepsize  $\mu_j = 0.65$  and stopping criteria  $\kappa = 0.999$ . Horizontal axis  $\delta$  and vertical axis  $\rho$  as defined in (1.2). Each transition is for  $n = 80$ , and the values of  $\rho$  shown are calculated using the average of  $r_{min}$  and  $r_{max}$ .

**3.2. Comparison of NIHT with NNM and PF.** Nuclear norm minimization (NNM), (1.4), is the convex relaxation of the rank minimization question (1.3) and is the most studied approach for matrix completion [9, 12, 38]. In particular, it is the only matrix completion formulation with a quantitatively accurate analysis [39] of the ability to recover the solution to (1.3). NNM can be formulated in terms of the well-studied SDP. There are many existing algorithms and software packages that can be used to solve (1.4); moreover, numerous algorithms have been designed to solve NNM specifically for matrix completion (see, for example, [5, 6, 41, 33]). These matrix completion focused methods for the solution of (1.4) are designed to more accurately and/or more rapidly return the solution, but they remain designed to give the solution to (1.4) and do not increase the range of the parameters  $\delta$  and  $\rho$  where the solution to (1.4) corresponds to that of (1.3). With our focus on determining the

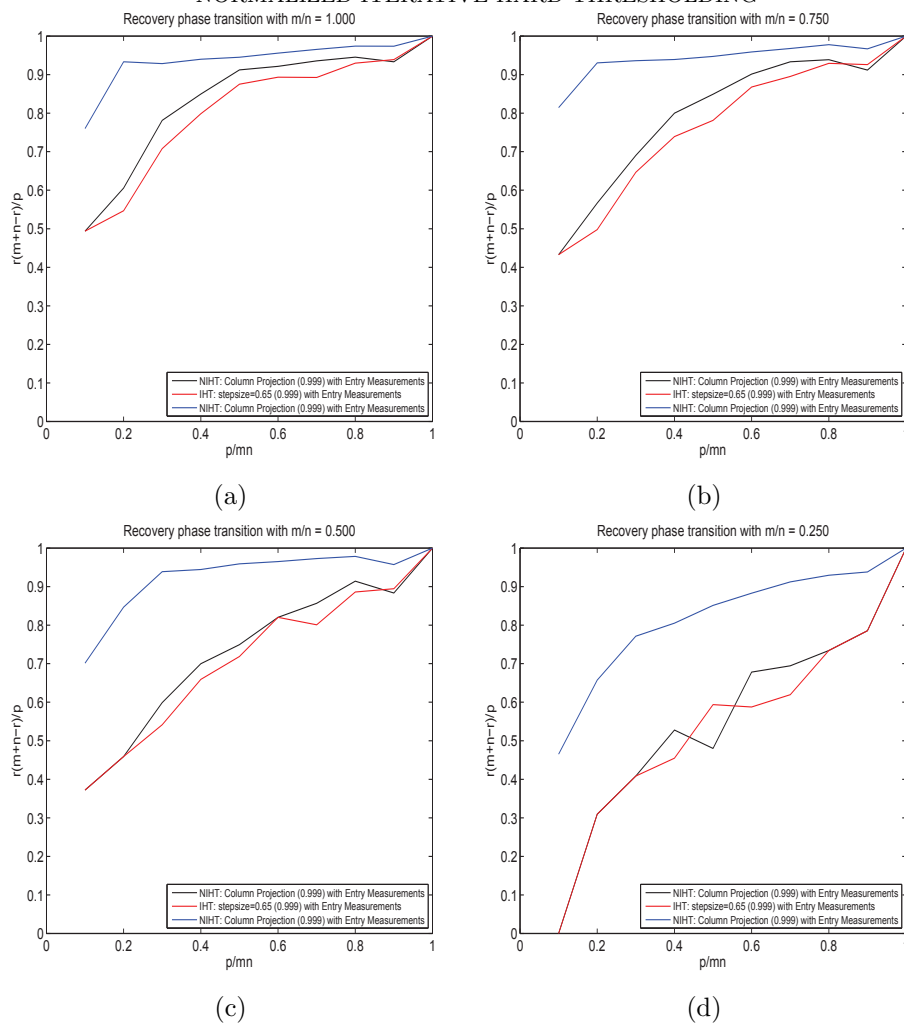


FIG. 3.2. Phase transition for entry sensing and algorithms: NIHT with column projection for  $n = 80$  (black) and  $n = 800$  (blue) and IHT with stepsize  $\mu_j = 0.65$  (red) with  $n = 80$ . Horizontal axis  $\delta$  and vertical axis  $\rho$  as defined in (1.2). The values of  $\rho$  shown are calculated using the average of  $r_{min}$  and  $r_{max}$ .

largest recoverable rank for an algorithm, we use the well-established software package SDPT3 [42] but are aware that specialized software is likely able to solve (1.4) in substantially less time. In addition to contrasting NIHT with NNM, we also compare NIHT with the very different manifold optimization method PowerFactorization (PF) [22]; see Algorithm 2.

PF seeks to directly solve the minimum rank problem (1.3) and is a particularly simple example of a class of methods [26, 45, 35] which are designed to remain on the manifold of rank  $r$  matrices throughout each iteration. Despite its simplicity, PF is capable of recovering matrices of surprisingly large rank. In contrast, NIHT updates the solution with directions that result in intermediate updates which are not on the manifold of rank  $r$  matrices; the algorithms presented in [43, 44, 28, 27, 40] are similar



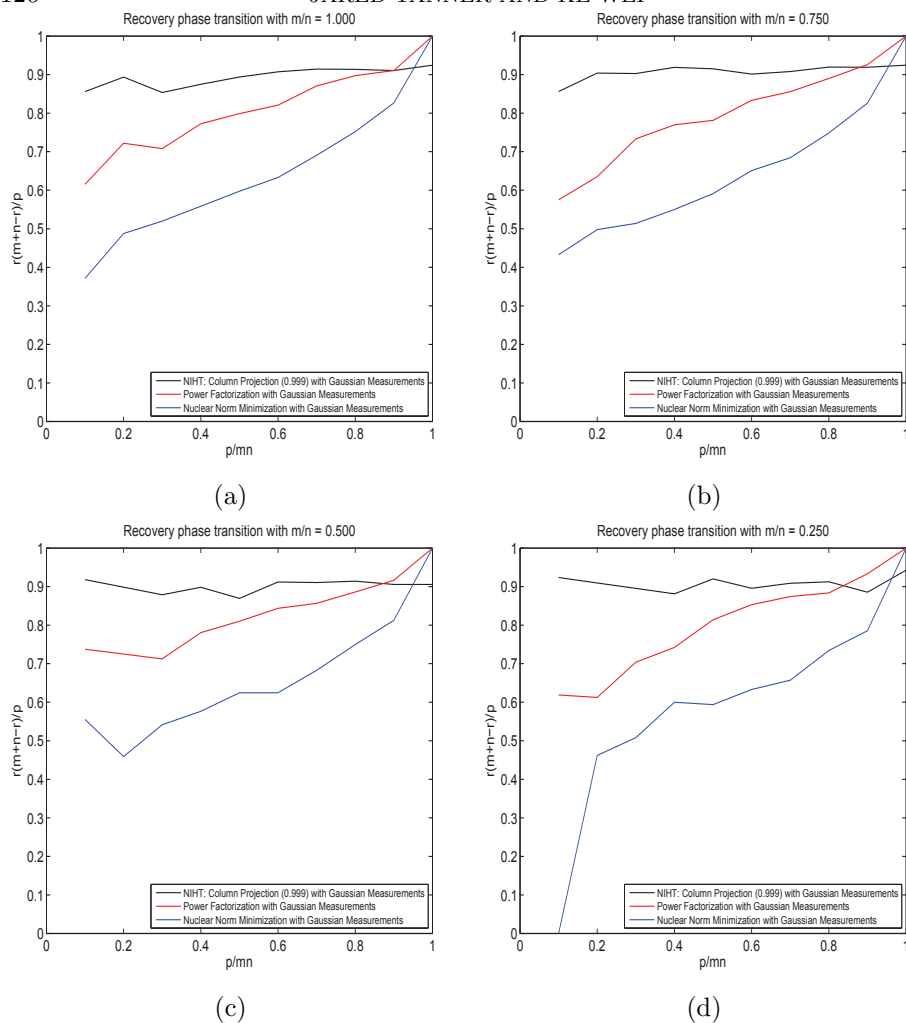


FIG. 3.3. Phase transition for Gaussian sensing and algorithms: NIHT, PF, and NNM, all with  $n = 80$ . Horizontal axis  $\delta$  and vertical axis  $\rho$  as defined in (1.2). The values of  $\rho$  shown are calculated using the average of  $r_{min}$  and  $r_{max}$ .

to NIHT in their use of (possibly restricted) descent directions of the measurement residual followed by projection onto the manifold of rank  $r$  matrices.

Figure 3.3 displays the phase transition for Gaussian sensing and NIHT (black), PF (red), and NNM (blue). NIHT and PF use the stopping criteria  $\kappa = 0.999$ , and SDPT3 uses a tolerance based stopping criteria to solve NNM. In every instance PF is observed to be able to recover matrices of larger rank than NNM can. NIHT is observed to be able to recover even larger rank for all but the largest values of  $\delta$ . The average timings for NNM and PF with  $m = n = 40$  are displayed in Figure 3.5 (f) and (h), respectively, and the ratio of their average timings as compared with NIHT is displayed in Figure 3.6 (d) and (f) for NNM and PF, respectively. NIHT is observed to be faster than NNM for all but  $\delta$  and  $\rho$  simultaneously large, where

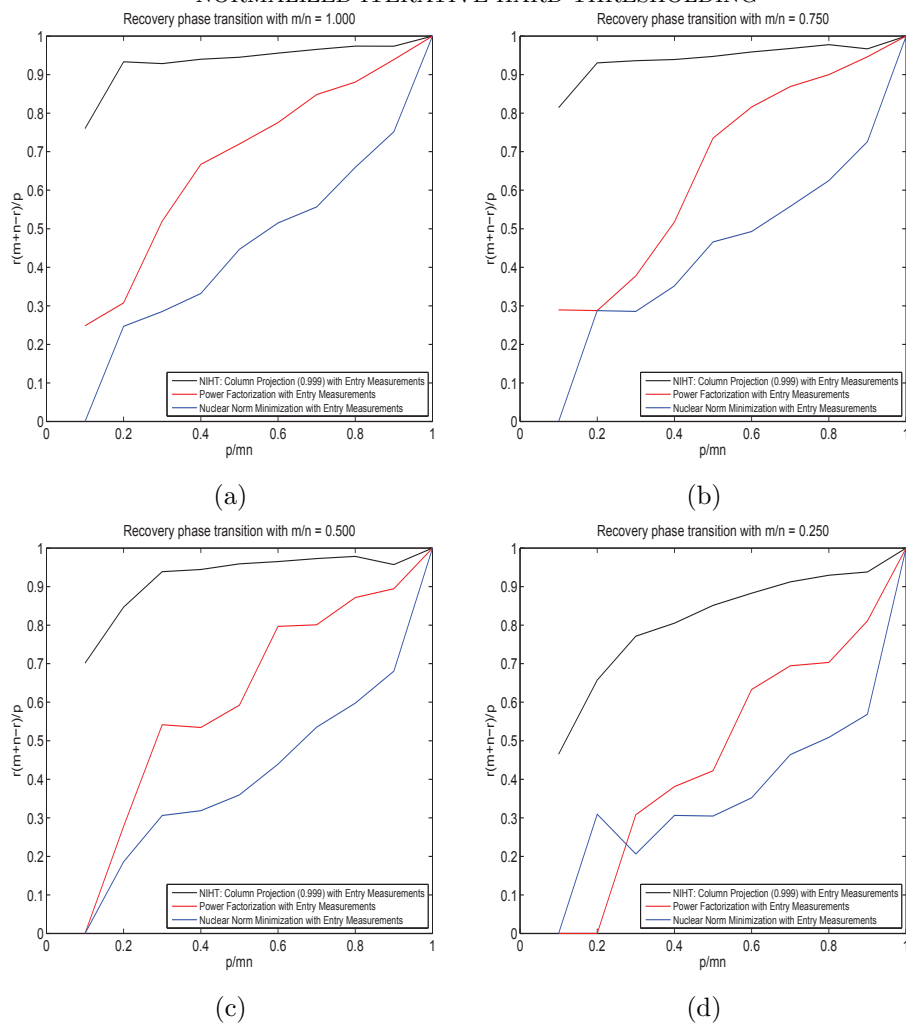


FIG. 3.4. Phase transition for entry sensing and algorithms: NIHT with  $n = 800$ , and NNM and PF both with  $n = 80$ . Horizontal axis  $\delta$  and vertical axis  $\rho$  as defined in (1.2). The values of  $\rho$  shown are calculated using the average of  $r_{min}$  and  $r_{max}$ .

NIHT is observed to be extremely slow. NIHT is observed to always be slower than PF for Gaussian sensing—typically three to seven times slower.

Figure 3.4 displays the phase transition for entry sensing and NIHT (black), PF (red), and NNM (blue). Again, NIHT and PF use the stopping criteria  $\kappa = 0.999$ , and SDPT3 uses a tolerance based stopping criteria. Memory requirements limit the size of problems that NNM and PF are able to solve to  $n = 80$ . In every instance NIHT is observed to be able to recover matrices of a larger rank than can PF, which is able to recover matrices of larger rank than can NNM. The average timings for NNM and PF for  $m = n = 80$  are displayed in Figure 3.5 (e) and (g), respectively, and the ratio of their average timings as compared with NIHT is displayed in Figure 3.6 (c) and (e) for NNM and PF, respectively. NIHT is observed to be faster than both NNM and PF—often more than ten times faster; however, it should be noted that

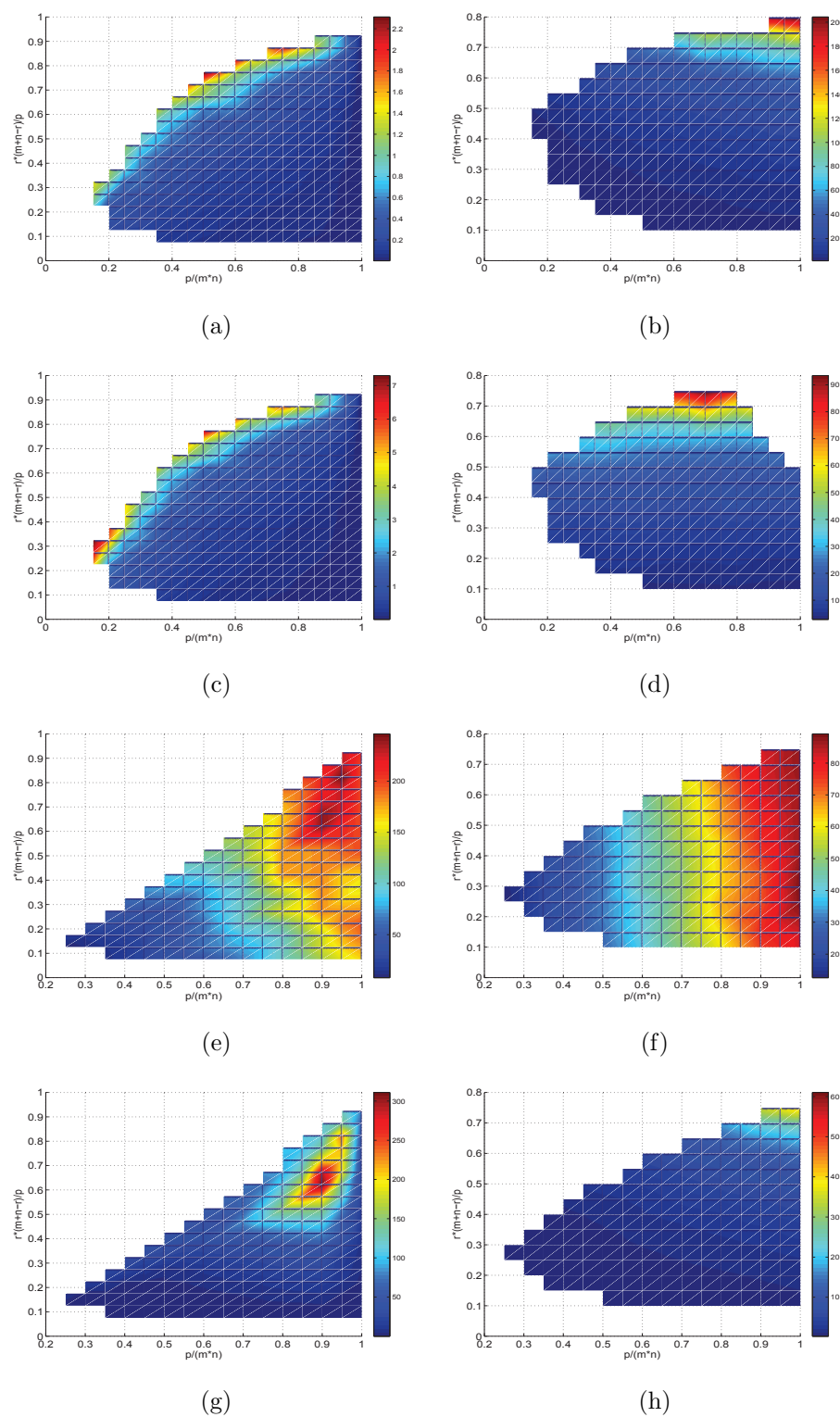


FIG. 3.5. Median time (seconds) for (a) NIHT with entry sensing, (b) NIHT with Gaussian sensing, (c) IHT with entry sensing, (d) IHT with Gaussian sensing, (e) NNM with entry sensing, (f) NNM with Gaussian sensing, (g) PF with entry sensing, and (h) PF with Gaussian sensing. Entry sensing tests are for  $m = n = 80$ , and Gaussian sensing tests are for  $m = n = 40$ . IHT uses the fixed stepsize  $\mu_j = 0.65$ .

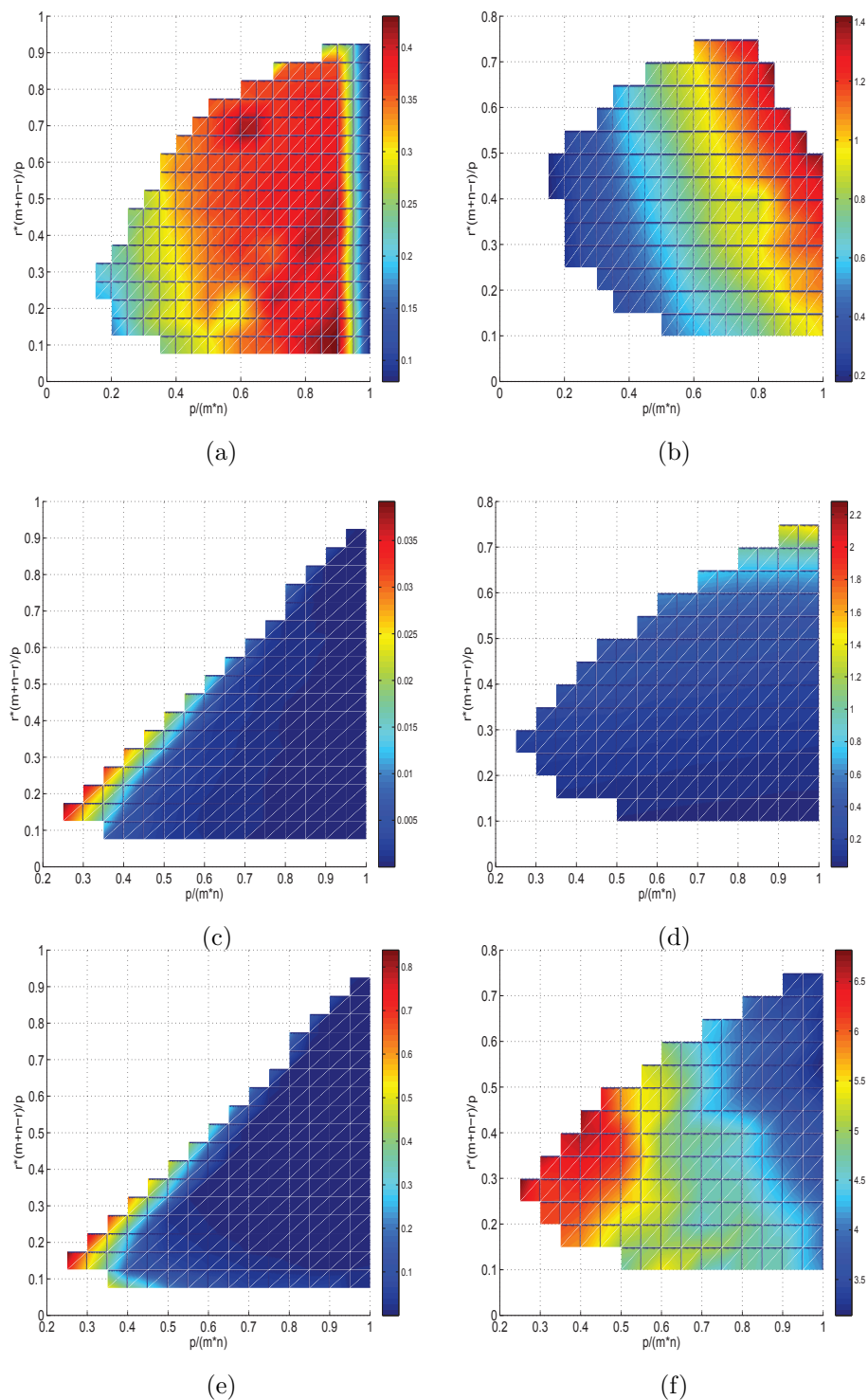


FIG. 3.6. Ratio of median time for NIHT divided by (a) IHT with entry sensing, (b) IHT with Gaussian sensing, (c) NNM with entry sensing, (d) NNM with Gaussian sensing, (e) PF with entry sensing, and (f) PF with Gaussian sensing. Entry sensing tests are for  $m = n = 80$ , and Gaussian sensing tests are for  $m = n = 40$ . IHT uses the fixed stepsize  $\mu_j = 0.65$ .

algorithms designed to solve (1.4) specifically for matrix completion can be expected to be substantially faster than that of SDPT3, and the use of iterative numerical linear algebra algorithms can be expected to accelerate PF.

**4. Conclusions.** Matrix completion is a seemingly very challenging problem that includes an infinite dimensional component lacking in compressed sensing. Despite this, even quite simple algorithms have the ability to recover a low rank matrix from only slightly more than the necessary number of linear measurements. NIHT is observed to be particularly effective; for the same number of measurements NIHT is typically able to recover matrices of rank higher than can NNM or PF. NIHT's ability to recover the largest rank matrices comes at the cost of allowing the method to converge at an extremely slow rate for the largest rank matrices. Neither PFN or NNM appear able to extend their recovery region in this way, though this may be possible for other algorithms related to NIHT, including [43, 44]. The ability to increase the recovery region at the cost of slow convergence rates suggests the need for accelerated variants of NIHT.

**Acknowledgments.** The authors thank the Institute for Mathematics and Its Applications (University of Minnesota) for their hospitality during the initial stages of this research. This work has made use of the resources provided by the Edinburgh Compute and Data Facility (ECDF).

#### REFERENCES

- [1] J. D. BLANCHARD, C. CARTIS, AND J. TANNER, *Compressed sensing: How sharp is the restricted isometry property?*, SIAM Rev., 53 (2011), pp. 105–125.
- [2] T. BLUMENSATH AND M. E. DAVIES, *Iterative hard thresholding for compressed sensing*, Appl. Comput. Harmon. Anal., 27 (2009), pp. 265–274.
- [3] T. BLUMENSATH AND M. E. DAVIES, *Normalized iterative hard thresholding: Guaranteed stability and performance*, IEEE J. Selected Topics Signal Process., 4 (2010), pp. 298–309.
- [4] A. M. BRUCKSTEIN, D. L. DONOHO, AND M. ELAD, *From sparse solutions of systems of equations to sparse modeling of signals and images*, SIAM Rev., 51 (2009), pp. 34–81.
- [5] J.-F. CAI, E. J. CANDÈS, AND Z. SUN, *A singular value thresholding algorithm for matrix completion*, SIAM J. Optim., 20 (2010), pp. 1956–1982.
- [6] J. F. CAI AND S. OSHER, *Fast Singular Value Thresholding without Singular Value Decomposition*, Tech. report, Rice University, Houston, TX, 2010.
- [7] E. J. CANDÈS, *Compressive sampling*, in Proceedings of the International Congress of Mathematics, Madrid, Spain, 2006, pp. 1433–1452.
- [8] E. J. CANDÈS, *The restricted isometry property and its implications for compressed sensing*, C.R. Math. Acad. Sci. Paris, 346 (2008), pp. 589–592.
- [9] E. J. CANDÈS AND B. RECHT, *Exact matrix completion via convex optimization*, Found. Comput. Math., 9 (2009), pp. 717–772.
- [10] E. J. CANDÈS, J. K. ROMBERG, AND T. TAO, *Stable signal recovery from incomplete and inaccurate measurements*, Comm. Pure Appl. Math., 59 (2006), pp. 1207–1223.
- [11] E. J. CANDÈS AND T. TAO, *Decoding by linear programming*, IEEE Trans. Inform. Theory, 51 (2005), pp. 4203–4215.
- [12] E. J. CANDÈS AND T. TAO, *The power of convex relaxation: Near-optimal matrix completion*, IEEE Trans. Inform. Theory, 56 (2009), pp. 2053–1080.
- [13] A. COHEN, W. DAHMEN, AND R. DEVORE, *Compressed sensing and best  $k$ -term approximation*, J. Amer. Math. Soc., 22 (2009), pp. 211–231.
- [14] W. DAI AND O. MILENKOVIC, *Subspace pursuit for compressive sensing signal reconstruction*, IEEE Trans. Inform. Theory, 55 (2009), pp. 2230–2249.
- [15] W. DAI, O. MILENKOVIC, AND E. KERMAN, *Subspace evolution and transfer (SET) for low-rank matrix completion*, IEEE Trans. Signal Process., 59 (2011), pp. 3120–3132.
- [16] D. L. DONOHO, *Compressed sensing*, IEEE Trans. Inform. Theory, 52 (2006), pp. 1289–1306.
- [17] D. L. DONOHO, *Neighborliness Polytopes and Sparse Solution of Underdetermined Linear Equations*, Tech. report, Stanford University, Stanford, CA, 2006.
- [18] D. L. DONOHO AND J. TANNER, *Precise undersampling theorems*, Proc. IEEE, 98 (2010), pp. 913–924.

- [19] Y. C. ELDAR, D. NEEDELL, AND Y. PLAN, *Unicity conditions for low-rank matrix recovery*, Appl. Comput. Harmon. Anal., 33 (2012), pp. 309–314.
- [20] S. FOUCART, *Hard thresholding pursuit: An algorithm for compressive sensing*, SIAM J. Numer. Anal., 49 (2011), pp. 2543–2563.
- [21] D. GOLDFARB AND S. MA, *Convergence of fixed-point continuation algorithms for matrix rank minimization*, Found. Comput. Math., 11 (2011), pp. 183–210.
- [22] J. P. HALDAR AND D. HERNANDO, *Rank-constrained solutions to linear matrix equations using power-factorization*, IEEE Trans. Signal Process. Lett., 16 (2009), pp. 584–587.
- [23] N. J. A. HARVEY, D. R. KARGER, AND S. YEKHANIN, *The complexity of matrix completion*, in Proceedings of the 17th Annual ACM-SIAM Symposium on Discrete Algorithms, ACM, New York, SIAM, Philadelphia, 2006, pp. 1103–1111.
- [24] P. JAIN, R. MEKA, AND I. DHILLON, *Guaranteed rank minimization via singular value projection*, in Proceedings of the Neural Information Processing Systems Conference (NIPS), Vancouver, Canada, 2010, pp. 937–945.
- [25] R. H. KESHAVAN, A. MONTANARI, AND S. OH, *Matrix completion from a few entries*, IEEE Trans. Inform. Theory, 56 (2010), pp. 2980–2998.
- [26] R. H. KESHAVAN AND S. OH, *Optspace: A gradient descent algorithm on the Grassmann manifold for matrix completion*, Tech. report, <http://arxiv.org/abs/0910.5260v2>, 2009.
- [27] A. KYRILLIDIS AND V. CEVHER, *Matrix ALPS: Accelerated low rank and sparse matrix reconstruction*, in Proceedings of the 2012 IEEE Statistical Signal Processing Workshop, IEEE, New York, 2012, pp. 185–188.
- [28] A. KYRILLIDIS AND V. CEVHER, *Matrix recipes for hard thresholding methods*, J. Math. Imaging Vision, April (2013), DOI: 10.1007/s10851-013-0434-7.
- [29] R. M. LARSEN, *PROPACK (software package)*, available online from <http://sun.stanford.edu/~rmunk/PROPACK/>.
- [30] K. LEE AND Y. BRESLER, *ADMiRA: Atomic decomposition for minimum rank approximation*, IEEE Trans. Inform. Theory, 56 (2010), pp. 4402–4416.
- [31] A. S. LEWIS AND J. MALICK, *Alternating projections on manifolds*, Math. Oper. Res., 33 (2008), pp. 216–234.
- [32] Z. LIN, M. CHEN, AND Y. MA, *The augmented Lagrange multiplier method for exact recovery of corrupted low-rank matrices*, Tech. report, <http://arxiv.org/abs/1009.5055>, 2010.
- [33] S. MA, D. GOLDFARB, AND L. CHEN, *Fixed point and Bregman iterative methods for matrix rank minimization*, Math. Program. Ser. A, 128 (2011), pp. 321–353.
- [34] A. MALEKI AND D. L. DONOHO, *Optimally tuned iterative reconstruction algorithms for compressed sensing*, IEEE J. Selected Topics Signal Process., 4 (2010), pp. 330–341.
- [35] G. MEYER, S. BONNABEL, AND R. SEPULCHRE, *Linear regression under fixed-rank constraints: A Riemannian approach*, in Proceedings of the 28th ACM International Conference on Machine Learning (ICML2011) (Bellevue, Washington), ACM, New York, 2011, pp. 545–552.
- [36] M. MICHENKOVA, *Numerical Algorithms for Low-Rank Matrix Completion Problems*, Tech. report, ETH, Switzerland, <http://www.math.ethz.ch/~kressner/students/michenkova.pdf>, 2011.
- [37] D. NEEDELL AND J. TROPP, *Cosamp: Iterative signal recovery from incomplete and inaccurate samples*, Appl. Comput. Harmon. Anal., 26 (2009), pp. 301–321.
- [38] B. RECHT, M. FAZEL, AND P. A. PARRILO, *Guaranteed minimum-rank solutions of linear matrix equations via nuclear norm minimization*, SIAM Rev., 52 (2010), pp. 471–501.
- [39] B. RECHT, W. XU, AND B. HASSIBI, *Null space conditions and thresholds for rank minimization*, Math. Program. Ser. B, (2011), pp. 175–211.
- [40] U. SHALIT, D. WEINSHALL, AND G. CHECHIK, *Online learning in the manifold of low-rank matrices*, Adv. Neural Inform. Process. Syst., 23 (2010), p. 2128–2136.
- [41] K. TOH AND S. YUN, *An accelerated proximal gradient algorithm for nuclear norm regularized least squares problems*, Pacific J. Optim., 16 (2010), pp. 615–640.
- [42] K. C. TOH, M. J. TODD, AND R. H. TÛTÛNCÛ, *SDPT3 4.0(beta) (software package)*, <http://www.math.nus.edu.sg/~mattohc/sdpt3.html>, 2006.
- [43] B. VANDEREYCKEN, *Low rank matrix completion by Riemannian optimization*, SIAM J. Optim., to appear.
- [44] B. VANDEREYCKEN AND S. VANDEWALLE, *A Riemannian optimization approach for computing low-rank solutions of Lyapunov equations*, SIAM J. Matrix Anal. Appl., 31 (2010), pp. 2553–2579.
- [45] Z. WEN, W. YIN, AND Y. ZHANG, *Solving a low-rank factorization model for matrix completion by a non-linear successive over-relaxation algorithm*, Math. Program. Comput., 4 (2012), pp. 333–361.